Reconstrução tomográfica a partir de projeções

EPUSP/PTC-5750
Sérgio S Furuie

Tomografia: secções de objetos

- Reflexão
  - Acústica: Ultra-som, Radar, ..
  - Ótica: microscópio confocal
- A partir das projeções
  - No domínio do espaço
    - transmissão : CT
    - emissão: SPECT, PET
  - No domínio da frequência
    - Ressonância Magnética (geometric projection, Fourier projection)

Tomografia a partir de projeções no espaço

- Conceito
  - Matemática da reconstruçao: Radon, 1917
- Aplicação
  - Astronomia: Bracewell, 1956
  - Medicina (revolução após Roentgen, 1895)
    - Primeiras publicações: Oldendorf, 1961
    - Primeiros experimentos: Kuhl (UPENN, 1963)
    - Equipamento médico: G Hounsfield (EMI, UK, 1971) e A Cormack (Tufts Univ) => Nobel, 1979

Estudo de caso: Phantom 3D

- background
- myocard.
- spots

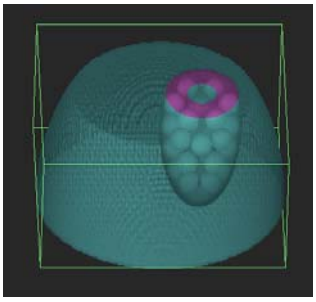

Dados disponíveis: Projeções

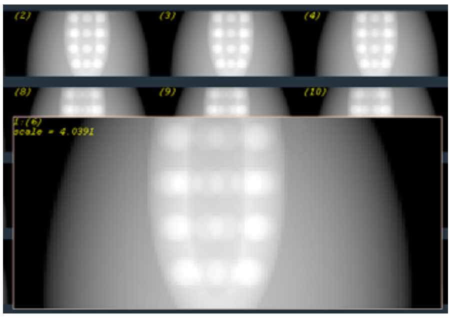

Processamento: Reconstrução

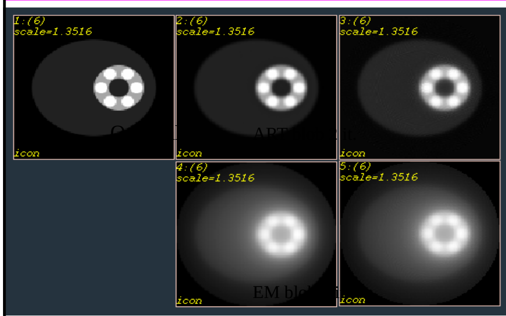

ART vox 2 it.

EM vox 2 it.

- Noiseless proj.

Motivação: 3D Reconstruction

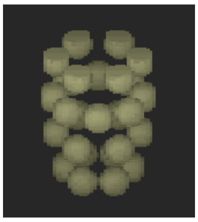

- ART Blob
- Noisyless data
- 2 iterations

Motivação: 3D rendering (surface)

- phantom
- segmentation
- surface rendering

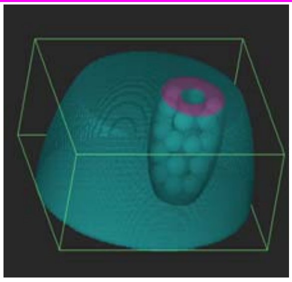

Motivation: Measuring in 3D

- distance
- area
- volume
- ejection fraction
- velocity
- ...

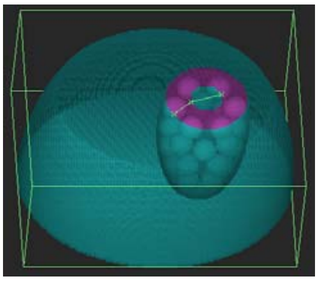

Reconst. Tomog. a partir de projeções

- Projection data formation
  - CT, spiral CT, multi-slice spiral CT (0.5 mm)^3, .5 s
  - SPECT
  - 3D PET
- Tomographic reconstruction methods
  - ML-EM : Maximum-likelihood
  - ART : Algebraic Reconstruction Technique
  - FBP : Filtered Backprojection
  - DFM : Direct Fourier Method

Gerações de tomógrafos por proj.

- Varredura de fonte unica e rotação da fonte-detetor
- Varredura de fonte conica e rotação
- Cone beam e rotação da fonte-detetor
  - spiral CT
  - multi-slice spiral CT
- Múltiplas fontes cônicas e detetores
- Electronic beam

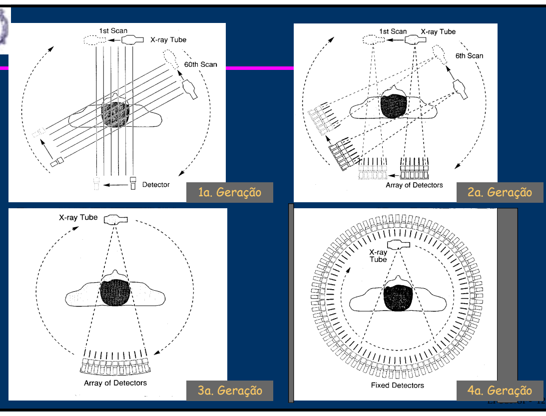

Multi-slice Spiral (helical) CT

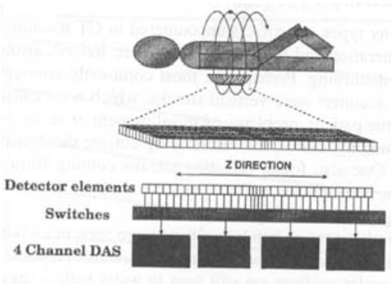

CT p/ Estruturas dinâmicas

- Ultrafast CT
  - sem estruturas móveis
  - 50 ms/scan (20 cortes/s)
  - volume: 8 cm em 0.25 s

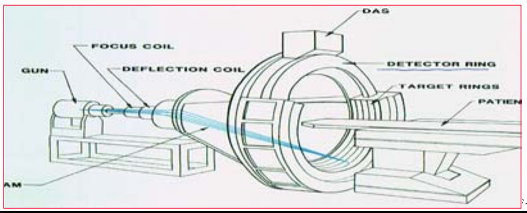

SPECT: Single Photon Emission CT

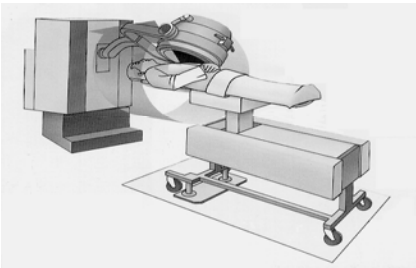

Tomografia por Transmissão (CT)

$$I = I_0 . \exp(-\int_L f(x,y).ds)$$

$$\ln(\frac{I_0}{I}) = \int_L f(x,y).ds \quad \text{(Integral de linha)}$$

$$g(t,\theta) = R\,f = \int_L f(x,y).ds$$

$$= \iint f(x,y).\delta(x.\cos\theta + y.\sin\theta - t).dx.dy$$

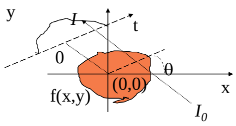

Transformada de Radon 2D
(projection operator)

f(x,y) ⟷ g(t,θ) (sinograma)

Solução?

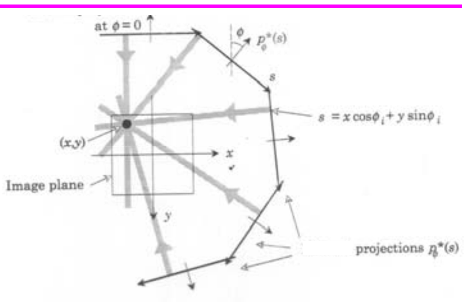

Reconstrução ingênua (backprojection)

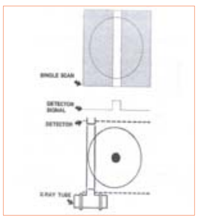

Reprojeção simples

Reconstrução com filtered backprojection

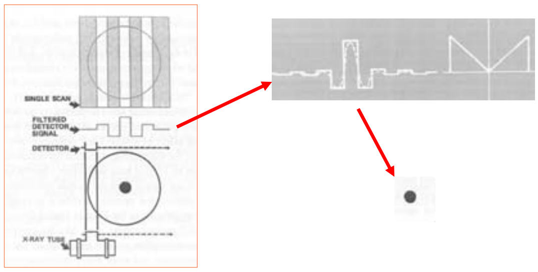

Algébrica

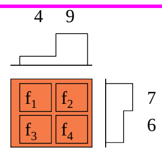

Imagem f

Problema: f |

$f_1 + f_2 = 7$

$f_3 + f_4 = 6$

$f_1 + f_3 = 4$

$f_2 + f_4 = 9$

Soluções

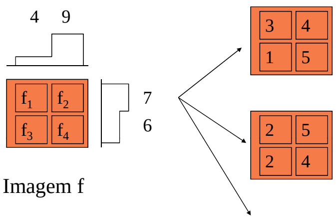

Imagem f

A . x = b

M equações com N incógnitas

Sistema indeterminado (infinitas soluções, rank < N)

Sistema inconsistente (M eq. Lin. Indep > N) => otimização

Algébrica: otimização (regularizada)

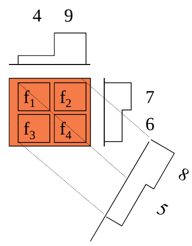

Imagem f

Problema: f |

$f_1 + f_2 = 7$

$f_3 + f_4 = 6$

$f_1 + f_3 = 4$

$f_2 + f_4 = 9$

$.5f_1 + f_3 + .5 f_4 = 5$

$.5f_1 + f_2 + .5 f_4 = 8$

Soluções (otimizada)

A . x = b

6 equações com 4 incógnitas

Sistema inconsistente (M eq. Lin. Indep > N) => otimização

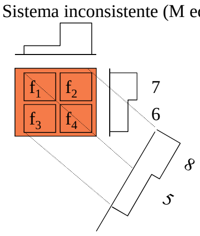

$$\min_{\hat{x}} | A.\hat{x} - b |^2$$

$$\hat{x} = A^+ b$$

$$A^+ = (A'A)^{-1} A'$$

→

2.5	4.6
2.0	4.1

Imagem f

Alguma outra solução ?

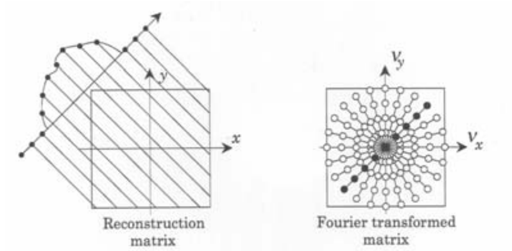

Teorema do corte central

Tomografia por Transmissão (CT)

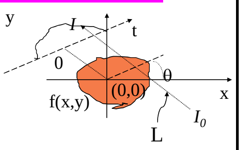

$$g(t,\theta) = R\ f = \int_L f(x,y).ds$$

$$= \iint f(x,y).\delta(x.\cos\theta + y.\sin\theta - t).dx.dy$$

Transformada de Radon 2D
(projection operator)

f(x,y) ⟷ g(t,θ) (sinograma)

Teorema da Projeção

$$g(t,\theta) = \iint f(x,y).\delta(x.\cos\theta + y.sin\theta - t).dxdy$$

$$G(u,\theta) \equiv \iint f(x,y) \int \delta(x.\cos\theta + y.sin\theta - t).e^{-j2\pi ut} dt.dxdy$$

$$G(u,\theta) = \iint f(x,y).e^{-j2\pi.u(x.\cos\theta + y.sin\theta)} dxdy$$

$$\therefore G(u,\theta) = F(u.\cos\theta, u.sin\theta) \Rightarrow \text{DFM}$$

Teorema da Projeção (cont.)

*Transf.Radon*Inversa

$$f(x,y) = \iint F(u,v).e^{j2\pi.(x.u+y.v)} du.dv$$

$$coord.polares \Rightarrow u = w.\cos\theta \quad \text{e } v = w.sin\theta$$

$$f(x,y) = \int_0^{2\pi} \int_0^{\infty} F_p(w,\theta).e^{j2\pi.(x.w.\cos\theta + y.wsin\theta)} w.dw.d\theta$$

$$f(x,y) = \int_0^{\pi} \int_{-\infty}^{\infty} F_p(w,\theta).e^{j2\pi.(x.w.\cos\theta + y.wsin\theta)} \,|w|.dw.d\theta$$

Reconstr. baseados em Transf.

- Direct Fourier Method
- Inverse Radon Transform
- Convolution Backprojection
- Filtered Backprojection
- Fan-beam
  - rebinning
  - fórmula

Ilustração DFM

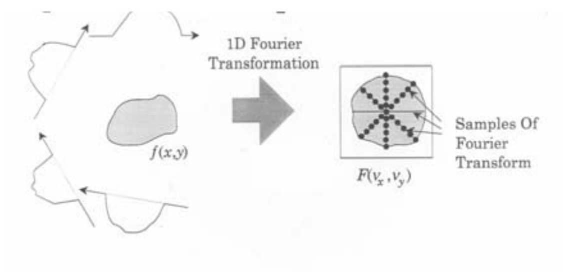

DFM : interpolação em freq.

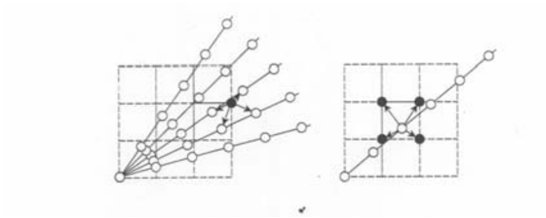

CBP, FBP

$$f(x,y)=\int_0^{\pi}\int_{-\infty}^{\infty}F_p(w,\theta).e^{j2\pi.(x.w.\cos\theta+y.w\sin\theta)}\,|w|.dw.d\theta$$

$$f(x,y)=\int_0^{\pi}\{\int_{-\infty}^{\infty}F_p(w,\theta).|w|.e^{j2\pi.w.(x.\cos\theta+y.\sin\theta)}dw\}.d\theta$$

$$f(x,y)=\int_0^{\pi}\hat{g}(x.\cos\theta+y.\sin\theta,\theta).d\theta$$

FBP

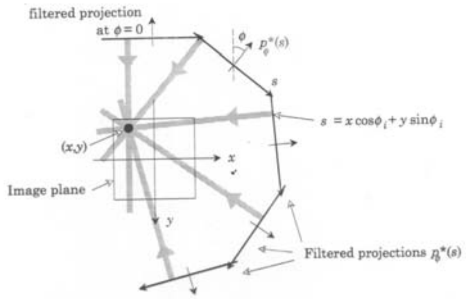

Normalização (escala Hounsfield)

$$H_{CT} = 1000\,\frac{\mu - \mu_{H_2O}}{\mu_{H_2O}}$$

$\therefore\ H_{CT}(\text{água}) = 0$

$H_{CT}(\text{ar}) = -1000$

$H_{CT}(\text{osso}) \cong 1000$

$\mu_{H_2O} = 0.190\ cm^{-1}(70\ kev)$

Massa branca e cinzenta: apenas alguns Hs

SPECT

$$p_i = \underbrace{\sum_j x_j.d_{ij}.A.\exp(-\int_{s_{ij}\to\infty}\mu_j(s)ds)}_{h_{ij}}$$

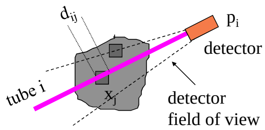

- Quantitative
  - EM
  - ART
- Approximate (Transform)
  - attenuation correction on projection data
  - attenuation correction on reconstructed data

$$\Rightarrow\ p_i = \sum_j h_{ij}.x_j$$

Solution: Algebraic Reconstruction

- System of linear equations
  - Huge system
  - Eg. volume: 64 x 64 x 64
    x_j j=1.. 262,144 voxels
  - Projections:
    128 views, 64x64 planes
    p_i i=1 .. 524,288 projs.
  - **H** : 524k x 262k
- Row-action methods
  - ART
  - EM

$p_i = \sum_j h_{ij}.x_j$ (all 3D projections)

$\vec{p} = \mathbf{H}.\vec{x}$ (vector notation)

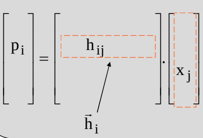

ART: Algebraic Reconst. Technique

- Noisy data
- Optimization criteria
  - Least-square solution
  - Minimum norm solution
    - row-action
    - relaxation

$\vec{p} = \mathbf{H}.\vec{x} + \vec{n}$

$$\vec{x}^{k+1} = \vec{x}^k + \lambda.\frac{p_i - \langle \vec{h}_i, \vec{x}^k \rangle}{||\vec{h}_i||^2}.\vec{h}_i$$

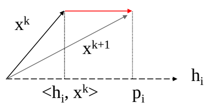

ART 3D: Algebraic Reconst. Techn.

- Noise removal: projection data estimation
- Quantitative reconstruction
- Fast (3D)
- Simple
- General
- [H] determination
- Stop criteria

EPUSP/SF - 41

Statistical Solution

- Projection: Poisson noise
- Maximum likelihood
  - Expectation-maximization algorithm
  - Iterative approach
- Maximum a posteriori
  - “a priori” probability distr.

$$\vec{p} = \text{Poisson}(\mathbf{H}.\vec{x})$$

$$\max_{\vec{x}} \Pr ob[\vec{p}|\vec{x}] \quad (ML)$$

$$\max_{\vec{x}} \Pr ob[\vec{x}|\vec{p}] \quad (MAP)$$

$$\Pr ob[\vec{x}|\vec{p}] = \frac{\Pr ob[\vec{p}|\vec{x}].\Pr ob[\vec{x}]}{\Pr ob[\vec{p}]}$$

EPUSP/SF - 42

Expectation-maximization

- Maximum Likelihood
- ML-EM algorithm

$$\max_{\vec{x}} \Pr ob[\vec{p}|\vec{x}]$$

$\Pr ob[\vec{p}|\vec{x}]$: independent Poisson

$$x_j^{k+1} = \frac{x_j^k}{\sum_i h_{ij}} \cdot \sum_i \frac{p_i}{< \vec{x}^k, \vec{h}_i >} h_{ij}$$

EPUSP/SF - 43

ML-EM

- Handles Poisson noise
- Total count conservation
- Convergence to ML
- Expectation-maximization
  - algorithm independent of rays direction
  - quantitative approach
  - iterative
  - slow convergence
  - no stop criterion

EPUSP/SF - 44

SPECT: Single Photon Emission CT

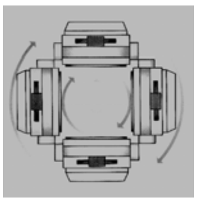

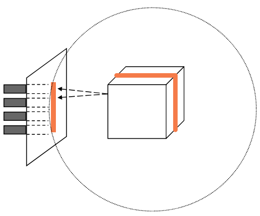

Conventional SPECT
- parallel collimator
- 2D reconstruction (slice-by-slice)

EPUSP/SF - 45

SPECT : parallel collimator

- Considering 2D effects
  - PSF
  - scattering
- Reconstruction approaches, slice-by-slice
  - EM
  - ART
  - 2D FBP

  (EM, ART: Quantitative)

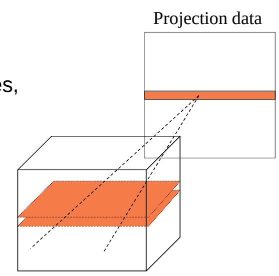

EPUSP/SF - 48

SPECT: Single Photon Emission CT

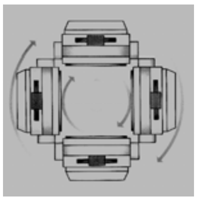

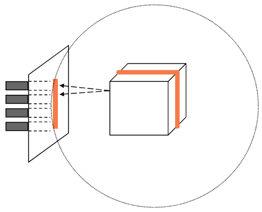

Conventional SPECT
- parallel collimator
- 2D reconstruction (slice-by-slice)

SPECT: projection data formation

- □ Parallel Collimators
  - stack of 2D slices
  - 3D effects of scattering
  - 3D effects of PSF

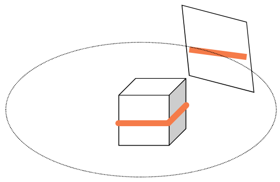

- □ Cone Beam collimators
  - 3D reconstruction (3D FBP)
  - improved sensitivity

SPECT : parallel collimator

- □ Considering 2D effects
  - PSF
  - scattering
- □ Reconstruction approaches, slice-by-slice
  - EM
  - ART
  - 2D FBP

(EM, ART: Quantitative)

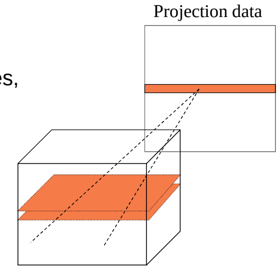

3D PET: Positron Emission Tomogr.

- □ Transversal and tilted lines
- □ Missing data

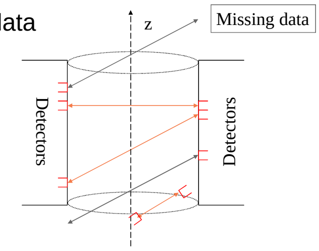

Projection data formation model (3D)

- □ General case (emission)

$$p_i = \sum_j x_j.\underbrace{(A.d_{ij})}_{vol_j}.\underbrace{\exp\left(-\int_{s_j}\mu_j(s)ds\right)}_{attenuation}$$

x_j : emission rate per unit volume

A : area of tube cross section

d_{ij} : intersection length

$\mu_j()$: attenuation function

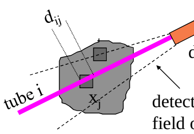

Emission CT (3D)

$$p_i = \sum_j x_j.(A.d_{ij}).\exp\left(-\int_{s_j}\mu_j(s)ds\right)$$

- □ 3D PET (quantitative)
  - scattering correction
  - attenuation correction
  - EM
  - ART
  - Transform methods

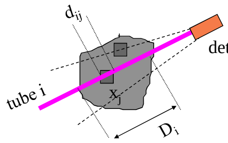

SPECT

$$p_i = \underbrace{\sum_j x_j . d_{ij} . A \exp\left(-\int_{s_{ij \to \infty}} \mu_j(s) ds\right)}_{h_{ij}}$$

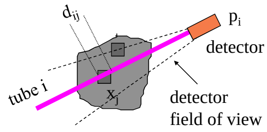

- Quantitative
  - EM
  - ART

$$\Rightarrow p_i = \sum_j h_{ij} . x_j$$

- Approximate (Transform)
  - attenuation correction on projection data
  - attenuation correction on reconstructed data

Single-slice rebinning

- 3D PET: multiple rings of detectors
  - Detection: intermediate slice
  - 2D FBP (slice-by-slice)
  - fast reconstruction
  - blur (axial aperture > 9 deg)
  - loss of resolution

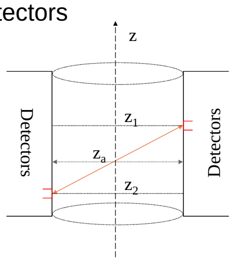

Multiple-slice rebinning

- 3D PET: multiple rings of detectors
  - detection: distributed along intermediate slices
  - deblurring along z-axis
  - quantitative approach

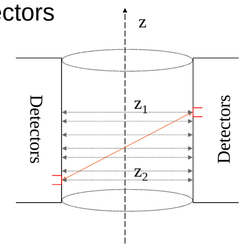

Tópicos

- Modelos de formação das projeções
- Reconstrução tomográfica 2D/3D
  - Aspectos gerais
  - Vantagens/desvantagens
- Métodos de reconstrução
  - Algébrico (ART)
  - Estatístico (ML-EM)
  - Analíticos
    - FBP, DFM
    - 3DRP, Favor, Cone
    - Simplificações: Rebinning

Bibliografia

- A.K. Jain, Fundamentals of Digital Image Processing, Prentice Hall, 1989.
- G.T. Herman, *Image Reconstruction from Projections*, Academic Press, 1980.
- J.C.Russ, The Image Processing Handbook, CRC Press, 1992.
- S.Matej, R.M.Lewitt, "Practical considerations for 3-D image reconstruction using spherically symmetric volume elements, IEEE Trans. Med.Imag., vol.15(1):68-78, Feb. 1996.
- L.A. Shepp, Y.Vardi "Maximum likelihood reconstruction for emission tomography", IEEE Trans.Med.Imag., vol.1(2):113-122, 1982.